Numerical analysis of stochastic relaxation in bistable systems driven by colored noise

T. Leiber, F. Marchesoni,* and H. Risken
Abteilung für Theoretische Physik, Universität Ulm, D-7900 Ulm, Federal Republic of Germany
(Received 4 January 1988)

The numerical analysis of stochastic relaxation in bistable periodic potentials driven by colored external noise is carried out by employing a numerical algorithm based on a well-established continued-fraction expansion. The present investigation is aimed to sort out conflicting theoretical predictions by providing a detailed and accurate numerical description of the phenomenon. Some of the perturbation theories reported in the literature are shown to reproduce, each to a different extent, the stationary probability distribution of the problem, whereas a nonperturbative approach is required to approximate the relevant relaxation time (mean first-passage time). Our numerical analysis exhibits the lack of a comprehensive theory of bistability in the presence of colored noise. A new finding of the study herein is the extension of the property of isospectrality of the Fokker-Planck equation under potential inversion (from bistable to metastable). Such a property is proved to hold for Fokker-Planck equations describing one-dimensional systems also driven by colored external noise.

I. INTRODUCTION

The determination of the mean first-passage time (MFPT) for bistable potentials plays a central role in a number of problems of statistical mechanics and synergetics.[1-3] For one-dimensional systems such a process is described by the stochastic differential equation

$$\dot{x} = -f'(x) + \epsilon(t) , \tag{1.1}$$

where $f(x)$ represents a bistable (nonlinear) potential and $\epsilon(t)$ an external Gaussian noise, the statistics of which has to be determined. In the white-noise limit the following correlation functions provide a complete description of the noise source:

$$\langle \epsilon(t) \rangle = 0, \quad \langle \epsilon(t)\epsilon(0) \rangle = 2D\delta(t) . \tag{1.2}$$

The Fokker-Planck equation (FPE) corresponding to the system represented by (1.1) and (1.2) has a simple form

$$\frac{\partial}{\partial t} P(x;t) = \frac{\partial}{\partial x} \left[f'(x) + D\frac{\partial}{\partial x} \right] P(x;t) , \tag{1.3}$$

and a number of its features are expressible analytically. In particular, the stationary probability distribution function $P_{\rm st}(x) = \lim_{t\to\infty}[P(x;t)]$ is independent of the initial conditions and reads

$$P_{\rm st}(x) = N \exp[-f(x)/D] , \tag{1.4}$$

where N is a suitable normalization constant. The MFPT, however, can be given an accurate analytical approximation, as first shown by Kramers in 1940.[4] Further refinements have been introduced over the years by a number of authors who specialized Kramers's approach to deal with more realistic physical conditions.[5,6]

An important effect which must be accounted for explicitly in order to attain a deeper insight into a variety of physical problems is the intrinsic noise menory. In our picture of many-body phenomena the noise source describes the heat bath of the irrelevant variables[2] which are assumed to have relaxed to equilibrium independent of the dynamics of the relevant variable $x(t)$. Any realistic heat bath, no matter how large the system volume, is characterized by at least one small relaxation time τ. The corresponding stochastic fluctuations are termed colored noise. The most common choice of time-correlated noise statistics is represented by

$$\langle \epsilon(t) \rangle = 0, \quad \langle \epsilon(t)\epsilon(0) \rangle = (D/\tau)\exp(-|t|/\tau) . \tag{1.5}$$

In spite of its apparent simplicity, the problem (1.1) and (1.5) is mostly unsolved. The stochastic differential equation (1.1) and Eq. (1.5) may be replaced by the two-dimensional system[1-3]

$$\begin{aligned} \dot{x} &= -f'(x) + \epsilon , \\ \dot{\epsilon} &= -(1/\tau)\epsilon + (1/\tau)\eta(t) , \end{aligned} \tag{1.6}$$

where $\eta(t)$ is a Gaussian external noise with correlation functions (1.2). In Eqs. (1.6) the time-correlated heat bath (1.5) has been replaced with a Markovian process $\epsilon(t)$ driven by a white noise $\eta(t)$. Such a procedure introduces some arbitrariness due to the choice of the sign of ϵ in the first equation (1.6). As a consequence, the invariance under parity $x \to -x$ which holds good for even potentials, $f(-x) = f(x)$, is broken. In many applications, however, the actual description of the system under study provides a natural symmetry-breaking mechanism.[6]

The FPE corresponding to Eq. (1.6),

$$\frac{\partial}{\partial t} P(x,\epsilon;t) = \mathbf{L}_{\rm FP}(x,\epsilon) P(x,\epsilon;t) , \tag{1.7}$$

$$\mathbf{L}_{\rm FP}(x,\epsilon) = \frac{\partial}{\partial x} f'(x) - \epsilon\frac{\partial}{\partial x} + \frac{1}{\tau}\frac{\partial}{\partial \epsilon}\left[\epsilon + \frac{D}{\tau}\frac{\partial}{\partial \epsilon} \right] , \tag{1.8}$$

does not admit of detailed balance.[3] As a result, the analytical expression for the stationary solution

$$P_{\rm st}(x,\epsilon)=\lim_{t\to\infty}[P(x,\epsilon;t)]$$

is *unknown*. In order to circumvent this difficulty a variety of approximations has been introduced in the literature.[7-19] The central idea consists in deriving a partial differential equation—in the form of an infinite expansion—for the reduced probability distribution function

$$P(x;t;\tau)=\int_{-\infty}^{\infty}P(x,\epsilon;t)d\epsilon\ , \tag{1.9}$$

so as to reproduce the static and some of the dynamical features of the FPE (1.7) and (1.8) up to the accuracy required. Such expansions are obtained from the full FPE on projecting out, adiabatically, the auxiliary variable ϵ.

It is often claimed that this kind of expansion, irrespective of the method employed for eliminating ϵ, would determine a perturbation expansion for $P(x;t;\tau)$ in the noise parameters D and τ. In practice, a reordering of the expansion terms according to powers of the perturbation parameters is not feasible because the terms generated at any step of the elimination procedure scale differently with respect to D and τ.[12-17] Finally, it must be remarked that the convergence of the adiabatic elimination is *not uniform in* x. This means that, for instance, we do not expect to achieve an equally good approximation to

$$P_{\rm st}(x;\tau)\equiv\lim_{t\to\infty}P(x;t;\tau)$$

in the whole x domain.

The results of the various expansion schemes can be summarized as follows. To the first step in the relevant adiabatic elimination procedure a *bona fide* FPE for $P(x;t;\tau)$ is recovered where both the drift function $G(x;\tau)$ and the diffusion function $D(x;\tau)$ may depend on the correlation time τ,

$$\frac{\partial}{\partial t}P(x;t;\tau)=\frac{\partial}{\partial x}\left[G(x;\tau)+\frac{\partial}{\partial x}D(x;\tau)\right]P(x;t;\tau)\ . \tag{1.10}$$

Although discrepancies among different approaches may look negligible at the lowest order, they affect markedly the determination of the related approximate stationary distribution $P_{\rm st}(x;\tau)$ (Refs. 7 and 9–13) and MFPT (Refs. 10 and 12–19). Three different forms of (1.10) reported in the literature are worth mentioning.

(i) τ *expansion* (Refs. 7 and 10). On employing different techniques, several authors derived the same form to be supposedly valid for *small* D *and* τ,

$$G(x;\tau)=f'(x),\quad D(x;\tau)=D[1-\tau f''(x)]\ . \tag{1.11}$$

Fox[10] has recently proposed a modified version of (1.11) which also applies in the *small*-τ limit only (functional-calculus method).

(ii) *Unified theory* (Ref. 11). Jung and Hänggi suggested a different form

$$G(x;\tau)=\{f'(x)+\tau Df'''(x)[1+\tau f''(x)]^{-2}\}\times[1+\tau f''(x)]^{-1}\ , \tag{1.12}$$
$$D(x;\tau)=D[1+\tau f''(x)]^{-2}\ ,$$

which is valid in the regime of small D and both *small and very large values of* τ, provided that

$$\gamma(x;\tau)=\frac{1}{\sqrt{\tau}}[1+\tau f''(x)]\gg\sqrt{D}\ |f''/f'|\ . \tag{1.13}$$

This condition may be fulfilled for monostable potentials uniformly in x, whereas for bistable potentials it may break down in the instability region, $f''(x)<0$, for moderate to strong noise color τ.[11]

(iii) *Decoupling ansatz* (Ref. 13). Hänggi and coworkers proposed an x-independent form of the diffusion function which would be particularly suitable for describing relaxation of bistable oscillators in the limit of *small* D (functional-derivative method),

$$D(\tau)=D/[1+\tau\langle f''(x)\rangle] \tag{1.14}$$

and $G(x;\tau)=f'(x)$. Here the average is to be taken over the unknown stationary distribution $P_{\rm st}(x;\tau)$ self-consistently.

The recent debate on the validity of the approximations (1.11)–(1.14) revealed the lack of rigorous results for the theoretical predictions to compare with. Up to now, the data available have been either plagued by too great an inaccuracy, as in the case of the digital simulation of Ref. 12, or forcibly limited to small barriers of the bistable potential $f(x)$. Both the analog simulation of Ref. 13 and the numerical solution discussed in Ref. 18 explore the relaxation process of a particular bistable system, namely, the quartic double-well potential, for barrier-height-to-noise intensity ratios up to 1. A significant comparison with theories (i)–(iii) would require, instead, an accurate numerical investigation for bistable potential coupled to colored noise with very small intensity.

This aim has been pursued in the present investigation. Our results are arranged as follows. In Sec. II we introduce a periodic version of the bistable potential and solve numerically the eigenvalue problem associated with the related FPE. Our numerical algorithm is outlined in the Appendix. In Sec. III the results for $P_{\rm st}(x;\tau)$ are reported for a wide range of parameter values. Comparison with the theoretical predictions (1.11)–(1.14) seems to suggest that the unified theory is the best candidate for reproducing the static properties of the system. In Sec. IV the smallest nonvanishing eigenvalue λ_1 of the FPE (1.7) and (1.8) is determined numerically. In the latter case, the most favorable comparison is obtained with predictions which may be reduced to the decoupling ansatz. In Sec. V it is proved that inverting the potential, i.e., $f(x)\to -f(x)$, does modify the stationary probability distribution but leaves the eigenvalue spectrum of the FPE unchanged, even in the nontrivial case when $\tau\neq 0$.

II. MODEL

Jung and Risken[18] investigated the stochastic relaxation in bistable potentials driven by colored noise by ad-

dressing the quartic double-well potential

$$f(x)=-(d_2/2)x^2+(d_4/4)x^4 , \tag{2.1}$$

which had been widely used in the literature. They also employed a matrix contained-fraction (MCF) expansion to solve the related FPE. The approach we followed in our investigation is very similar, but for the choice of the potential function. In our case,

$$f(x)=-a\cos(x)+b\cos(2x) , \tag{2.2}$$

with $a,b>0$, $a<4b$. In Ref. 18 natural boundary conditions are assumed, i.e.,

$$\lim_{x\to\pm\infty}[P(x,\epsilon;t)]=0 .$$

For a periodic potential the periodicity condition

$$P(x+2\pi,\epsilon;t)=P(x,\epsilon;t) \tag{2.3}$$

is needed to normalize the probability distribution function to one particle per period. Potential (2.2) is plotted in Fig. 1 for the one-period interval $[-\pi,\pi]$. (For a recent application of the potential (2.2) in the context of nonequilibrium phase transitions and biological ordering phenomena, see, eg., Ref. 20.)

The advantage of the present choice for $f(x)$ can be appreciated when one looks at the main features of the MCF algorithm. On making the ansatz

$$P(x,\epsilon;t)=P(x,\epsilon)\exp(-\lambda t) ,$$

the FPE (1.7) is turned into an eigenvalue problem,

$$-\lambda P(x,\epsilon)=\mathbf{L}_{\rm FP}(x,\epsilon)P(x,\epsilon) , \tag{2.4}$$

with $\lambda\geq 0$. The symmetry $\mathbf{L}_{\rm FP}(x,\epsilon)=\mathbf{L}_{\rm FP}(-x,-\epsilon)$ allows us to separate $P(x,\epsilon)$ into an odd and an even part,

$$P(x,\epsilon)=P^o(x,\epsilon)+P^e(x,\epsilon) , \tag{2.5}$$

$$\begin{aligned} P^o(x,\epsilon)&=\Psi_0(\epsilon)\sum_{m,n\geq 0}[c^n_{2m}\sin(nx)\Psi_{2m}(\epsilon) \\ &\quad +c^n_{2m+1}\cos(nx)\Psi_{2m+1}(\epsilon)] , \\ P^e(x,\epsilon)&=\Psi_0(\epsilon)\sum_{m,n\geq 0}[c^n_{2m}\cos(nx)\Psi_{2m}(\epsilon) \\ &\quad +c^n_{2m+1}\sin(nx)\Psi_{2m+1}(\epsilon)] . \end{aligned} \tag{2.6}$$

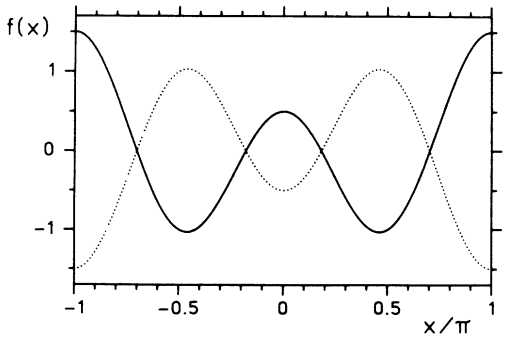

FIG. 1. Solid curve, *bistable periodic* potential (2.2) with $a=0.5$ and $b=1$. Dotted curve, *metastable periodic* potential (2.2) with $a=-0.5$ and $b=-1$.

Here $\Psi_m(\epsilon)$ are normalized Hermite functions and $\Psi_0(\epsilon)\Psi_m(\epsilon)$ are the eigenfunctions of the bath operator

$$\mathbf{L}_B(\epsilon)=\frac{1}{\tau}\frac{\partial}{\partial\epsilon}\left[\epsilon+\frac{D}{\tau}\frac{\partial}{\partial\epsilon}\right] , \tag{2.7}$$

with eigenvalue m/τ. Depending on the quantity we want to determine, we only need to take into account either the even or the odd part of $P(x,\epsilon)$. Susbtituting Eq. (2.6) into Eq. (2.4) accordingly and truncating the double sum in $P^{o,e}$ at $n=N$ and $m=M$ yields a homogeneous tridiagonal vector recurrence relation[3,19]

$$\mathbf{Q}^+_m\mathbf{c}_{m+1}+\mathbf{Q}_m\mathbf{c}_m+\mathbf{Q}^-_m\mathbf{c}_{m-1}=0 , \tag{2.8}$$

where $\mathbf{Q}^+_m=-\mathbf{Q}^-_{m+1}$ and $\mathbf{Q}_m$ are the matrices which are reported in the Appendix, and $\mathbf{c}_m=\{c^n_m\}$ denote the expansion coefficients of Eq. (2.6). On defining the matrices $\mathbf{K}_m$, $\mathbf{K}_m\mathbf{c}_m\equiv\mathbf{Q}^+_m\mathbf{c}_{m+1}$, Eq. (2.8) can be cast into the form of a MCF (Refs. 3 and 19) with the initial condition that $\mathbf{K}_M=0$, which corresponds to setting $\mathbf{c}_m=\mathbf{0}$ for $m=M+1$. Computation of the eigenvalue spectrum is thus reduced to the solution of the determinantal equation

$$\det[\mathbf{Q}_0(\lambda)+\mathbf{K}_0(\lambda)]=0 . \tag{2.9}$$

The corresponding eigenfunctions can also be computed by summing up the relevant series in Eq. (2.6), its coefficients being determined numerically through the matrices $\mathbf{K}_m$, see Ref. 21. A detailed account of the numerical algorithm employed in the present investigation is given in the Appendix.

Jung and Risken[18] expanded $P(x,\epsilon)$ in a similar way. The most convenient set of orthogonal x functions compatible with the natural boundary conditions in the quartic double-well problem proved to be $H_n(x)=\Psi_0(x)\Psi_n(x)$ with $\Psi_n(x)$ again representing the normalized Hermite functions. As the Fourier series (2.6) converges much faster than the expansion of Ref. 18, the choice of a periodic potential, Eq. (2.2), enables us to explore the properties of stochastic relaxation in bistable systems for a much larger range of the noise parameters D and τ. Very recently, Jung and Hänggi[22] modified the biorthogonal expansion for the quartic double-well potential, thus improving on the convergence of the MCF. Therefore, in Ref. 22 a quite remarkable extension of the relevant parameter ranges, compared to those of Ref. 18, was achieved.

It might be noted, however, that our choice of the potential function can approximate fairly closely the structure of a characteristic double-well potential. In Fig. 1 the potential $f(x)$ exhibits two barriers, a higher one at $x=\pm\pi$ and a lower one at $x=0$. The barrier heights are

$$\begin{aligned} \Delta f(\pi)&=2b+a+\frac{a^2}{8b} , \\ \Delta f(0)&=2b-a+\frac{a^2}{8b} , \end{aligned} \tag{2.10}$$

respectively. If a and b are taken so that $\Delta f(\pi)\gg\Delta f(0)$, the escape rate across the boundaries $x=\pm\pi$ is negligible compared to the escape over the bar-

rier at $x=0$. In view of the periodicity condition (2.3), we have a *periodic bistable potential.* Furthermore, we remark that the MFPT over high-potential barriers, $\Delta f(0) \gg D$, is mostly determined[4,5] by the ratio $\Delta f(0)/D$ and the second derivatives of the potential function about the minima $\pm x_m$ and the barrier $x_M=0$, respectively. In our case ($a<4b$),

$$f''(\pm x_m)=4b-\frac{a^2}{4b}\ ,$$
$$|f''(x_M=0)|=4b-a\ . \tag{2.11}$$

The exact shape of the potential function for given values of $\Delta f(0)/D$, $f''(x_m)$, and $|f''(0)|$ contributes to determining the MFPT at higher orders in $D/\Delta f(0)$. Small corrections might also arise due to the presence of the (higher) barrier located in $x=\pm\pi$.[21]

For the sake of comparison with the quartic double-well potential,[18] we display in Fig. 2 the stationary distribution $P_{\rm st}(x;\tau)$ for our system. The potential parameters a and b have been chosen in order to best reproduce the shape of the quartic double-well potential studied by Jung and Risken.[18] In particular, the ratio $\Delta f(0)/D$ and the curvature at the potential minima $f''(x_m)$ coincide exactly in the two cases, whereas $|f''(0)|$ takes the value 1.0 for their potential and 1.25 for ours. The stationary distributions for the two potentials are almost identical (see Ref. 18, Fig. 2). Small deviations are mostly due to the different boundary conditions. Further calculations show that the corresponding first nonvanishing eigenvalue employed in Ref. 18, Fig. 6, compares also very well. However, it should be noted that in computing $P_{\rm st}(x;\tau)$ we easily achieved a good numerical convergence over the whole x domain for values of $\Delta f(0)/D$ and τ up to 3.0, while the relevant upper bounds in Ref. 18 are 0.5 and 1.0, respectively.

III. STATIONARY DISTRIBUTION $P_{\rm st}(x;\tau)$

As discussed in Sec. I it is desirable to study numerically the steady state of the system under investigation in order to sort out conflicting predictions reported in the literature. Our results for $P_{\rm st}(x;\tau)$ are displayed in Fig. 3 for different values of the parameters D and τ. We immediately note the following.

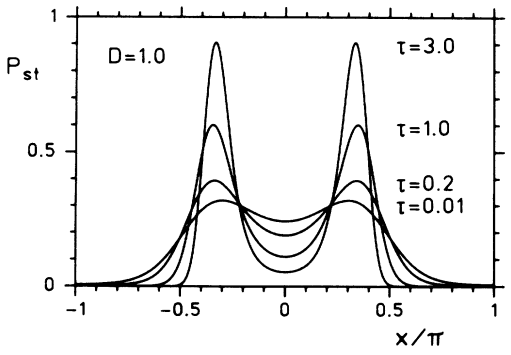

FIG. 2. Stationary distribution $P_{\rm st}(x;\tau)$ for the bistable periodic potential (2.2) with $a=\frac{15}{8}$ and $b=\frac{25}{32}$, i.e., $\Delta f(0)=0.25$, $\Delta f(\pi)/\Delta f(0)=16$.

(i) $P_{\rm st}(x;\tau)$ is a symmetric two-peaked function. Such a peak structure is enhanced for large correlation times, i.e., the peaks get narrower and higher.

(ii) The positions of the peak maxima $\pm x_p$ coincide with the potential minima $\pm x_m$ at $\tau=0$. As τ increases, the peaks shift symmetrically to larger (absolute) values of x, $x_p>x_m$. For very large τ this trend is reversed and the two peaks come close to the potential minima $\pm x_m$ again. The absolute value of the peak shift for the parameter values adopted in Fig. 3 is less than 1% and therefore hard to detect by inspection. The dependence of the quantity $\delta=x_p-x_m$ on τ is illustrated in Fig. 4.

For the sake of comparison we report the analytical expressions of $P_{\rm st}(x;\tau)$ as predicted by the three approximated theories outlined in Sec. I.

(i) τ *expansion* (Refs. 7 and 10) (D and τ small),

$$P_{\rm st}(x;\tau)=\frac{N}{|1-\tau f''(x)|}\times\exp\left[-(1/D)\int_0^x\frac{f'(y)}{1-\tau f''(y)}dy\right]. \tag{3.1}$$

(ii) *Unified theory* (Ref. 11) [D small and $\gamma(x;\tau)\gg\sqrt{D}\,|f''/f'|$, see Eq. (1.13)],

$$P_{\rm st}(x;\tau)=N|1+\tau f''(x)|\times\exp\left[-\frac{f(x)}{D}-\frac{\tau}{2D}f'^2(x)\right]. \tag{3.2}$$

(iii) *Decoupling ansatz* (Ref. 13) (D small),

$$P_{\rm st}(x;\tau)=N\exp\left[\frac{-f(x)}{D}[1+\tau\langle f''(x)\rangle]\right]. \tag{3.3}$$

The average $\langle f''(x)\rangle$ is taken with respect to $P_{\rm st}(x;\tau=0)$, and N are suitable normalization constants. In Fig. 3 our numerical data are plotted against the theoretical predictions (3.1)–(3.3). The range of applicability of the theoretical approaches is clearly illuminated by these curves.

We see immediately that the τ expansion (3.1) approximates adequately the reduced stationary distribution $P_{\rm st}(x;\tau)$ for small noise parameters D and very weak noise color τ [Fig. 3(a)]. However, the prefactor in Eq. (3.1) determines the overshoot of the peaks in the corresponding curves even for relatively small values of τ and small D [Fig. 3(b)]. The analytical form for $P_{\rm st}(x;\tau)$ obtained by means of the τ expansion Eq. (3.1) diverges at the points $\pm\bar{x}$ where the diffusion function vanishes, i.e., $D(\bar{x},\tau)=0$. For the periodic potential (2.2) this can only occur when $1/\tau<f''(x_m)=4b-a^2/(4b)$. Under such circumstances $\pm\bar{x}$ act as reflecting walls for the solution of the *bona fide* FPE (1.10) and (1.11).[3] The decoupling ansatz, on the contrary, reproduces $P_{\rm st}(x;\tau)$ fairly closely for small values of D and moderate to large values of τ. However, for increasing noise color τ the peaks of the stationary probability density are underestimated [Fig. 3(c)]. This trend and the absence of peak shifting is confirmed for larger values of D [Figs. 3(e) and 3(f)] which, anyway, lie well beyond the range of applicability of the decoupling ansatz.

The unified theory reproduces our numerical results for $P_{st}(x;\tau)$ rather accurately for small-D values in the whole range of noise color τ considered [Figs. 3(a)–3(c)]. As a matter of fact, prediction (3.2) breaks down (as expected, see Ref. 11) in the instability region about the potential barrier [Figs. 3(c) and 3(f)]. The inverting points $\pm\bar{x}(\tau)$ which restrict the instability region about the two barriers are defined by the equations $D(\bar{x};\tau)=\infty$, with $D(x;\tau)$ given by Eqs. (1.12) and (1.13). Thus, there exist no inverting points if $-f''(x)<1/\tau$ holds in the whole x interval. The onset of the breakdown of prediction (3.2) is determined by the lowest value of $f''(x)$ in the interval, for our potential $f''(\pm\pi)=-4b-a=-4.5$. In other words, the first instability occurs about the higher barrier for $\tau=\frac{2}{9}$. When τ exceeds this value the instability region about the higher barrier grows, and for $\tau>\frac{2}{7}$ a second instability region about the lower barrier appears. For values of τ large enough, the inverting points define distinct disconnected support domains for the distribution (3.2). Under such circumstances the most favorable comparison with our numerical data has been achieved on normalizing the distribution function symmetrically on the allowed x intervals about the potential minima. In the instability regions $P_{st}(x;\tau)$ has been set to zero [Figs. 3(c) and 3(f)].

In Fig. 4 we plotted the peak shift $\delta(\tau)=x_p(\tau)-x_m$ versus τ for different values of D. The log-log scale has been chosen to exhibit the linear increase of $\delta(\tau)$, for small values of τ, and its inverse proportional decrease for large values of τ. As a matter of fact, neither the τ ex-

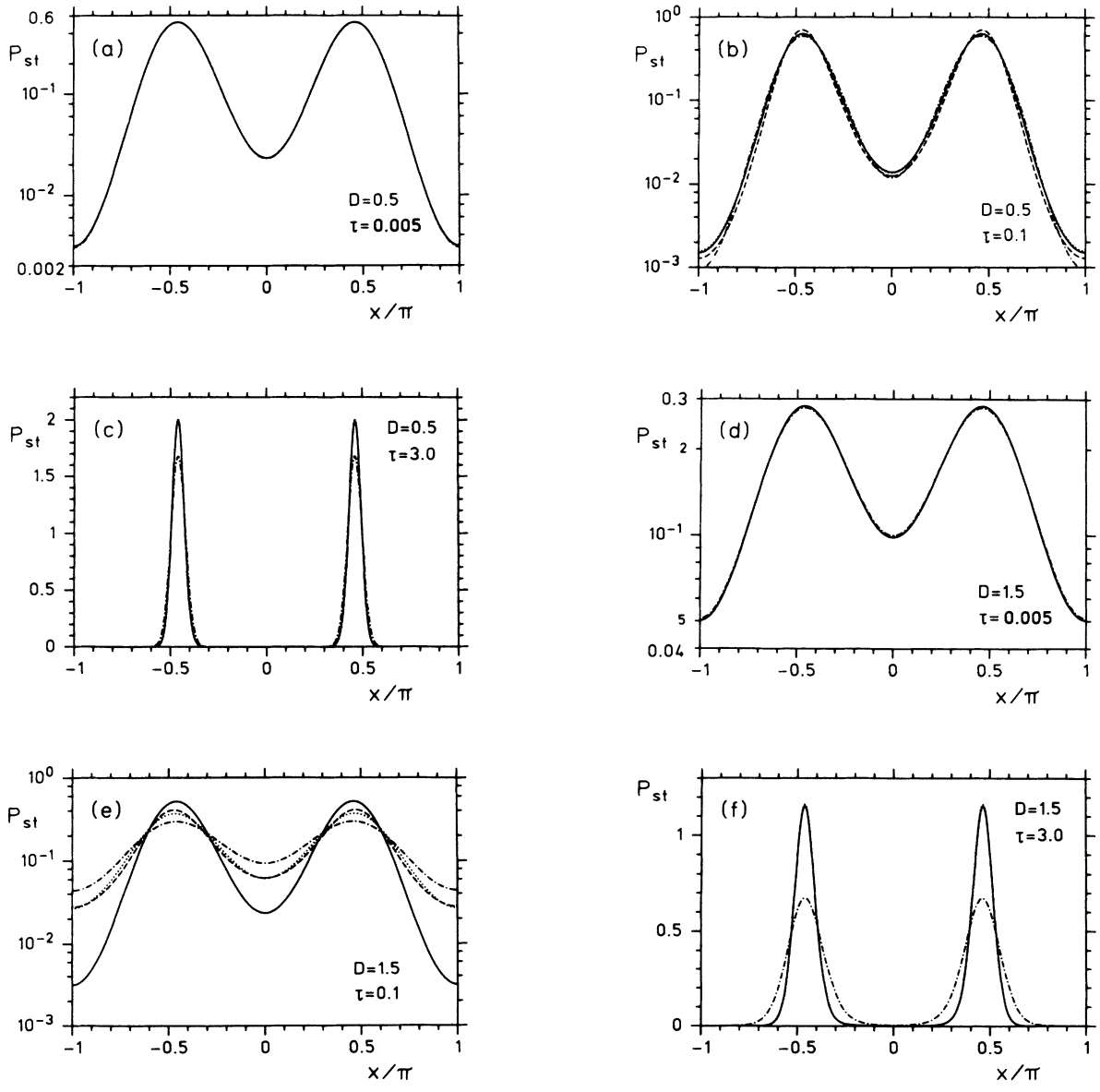

FIG. 3. (a)–(f), stationary distribution $P_{st}(x;\tau)$ for the *bistable periodic* potential (2.2) with $a=0.5$ and $b=1$, i.e., $\Delta f(0)=\frac{49}{32}$, $\Delta f(\pi)/\Delta f(0)=\frac{81}{49}$. Solid curves, MCF result. Dotted curves, unified theory. Dashed curves, τ expansion. Dotted-dashed curves, decoupling ansatz. (c) and (f), linear scale; others, logarithmic scale.

pansion[7,10] nor the decoupling ansatz[13] reproduces the peak shift. However, the prediction of the unified theory for $x_p(\tau)$ can be easily derived by imposing the condition that $(\partial/\partial x)P_{st}(x;\tau)=0$.

From Eq. (3.2) we obtain

$$D\tau f'''(x_p)-f'(x_p)[1+\tau f''(x_p)]^2=0 . \tag{3.4}$$

For the sake of comparison with the MCF results, we solved Eq. (3.4) numerically and displayed the corresponding peak shift $\delta(\tau)$ in Fig. 4. Since, in our computations, δ is very small compared to x_m, we may expand each term on the left-hand side of Eq. (3.4) about $\pm x_m$ and solve with respect to δ analytically,

$$\delta(\tau)=\frac{D\tau f^{(3)}(\pm x_m)}{f^{(2)}(x_m)[1+\tau f^{(2)}(x_m)]^2-D\tau f^{(4)}(x_m)} . \tag{3.5}$$

The compact notation $f^{(n)}(x)$ denotes the nth derivative of $f(x)$ with respect to x. For our potential

$$f^{(3)}(\pm x_m)=\pm 3a[1-(a/4b)^2]^{1/2} ,$$

$$f^{(4)}(x_m)=-16b\left[1-\frac{7a^2}{64b^2}\right] ,$$

and $f^{(2)}(x_m)$ is given in Eq. (2.11). In the asymptotic regimes Eq. (3.5) simplifies as follows:

$$\delta(\tau)=D\tau\frac{f'''(\pm x_m)}{f''(x_m)}, \quad \tau f''(x_m)\ll 1 \tag{3.6}$$

and

$$\delta(\tau)=(D/\tau)\frac{f'''(\pm x_m)}{f''^{3}(x_m)}, \quad \tau f''(x_m)\gg 1 . \tag{3.7}$$

For the parameter values of Fig. 4, the analytical expression (3.5) and the exact numerical determination of $\delta(\tau)$ obtained from Eq. (3.4) coincide almost identically. In our derivation of $\delta(\tau)$ we assumed that $\gamma(x;\tau)$ does not change sign. This is a reasonable assumption everywhere in the x domain apart from the region of instability. For very large correlation times the stationary distribution tends to peak about the potential minima, as shown in Figs. 2 and 3. The stationary distribution $P_{st}(x;\tau)$ is therefore concentrated in two small intervals about $\pm x_m$, where $f''(x)$ is positive definite. The lack of uniform convergence for $P_{st}(x;\tau)$ in the instability region also explains why prediction (3.5) does not work too well for very large values of D (Figs. 3 and 4).

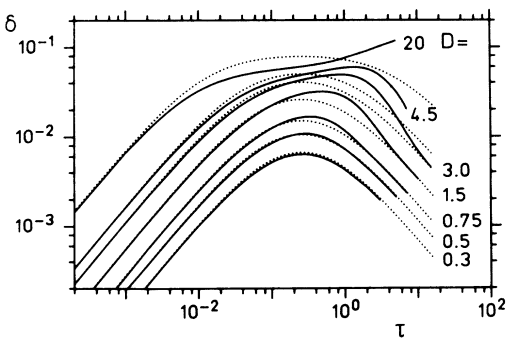

FIG. 4. Peak shift $\delta(\tau)$ of the stationary distribution $P_{st}(x;\tau)$ for the *bistable periodic* potential (2.2) with $a=0.5$ and $b=1$. Solid curves, MCF result. Dotted curves, unified theory approximation.

Recently, Altares and Nicolis[9] developed a large-τ perturbation approach in the dimensional order parameter $D/(b^3\tau^2)$ (in our units). In their scheme the peak shift is given by

$$\delta_{AN}(\tau)=\frac{D\tau f'''(\pm x_m)}{[1+2\tau f''(x_m)][1+(\tau/2)f''(x_m)]f''(x_m)} . \tag{3.8}$$

Their result differs from Eq. (3.5) essentially in that the D dependence in the denominator has been suppressed. As a consequence, Eq. (3.8) does reproduce the limiting cases of the unified theory, (3.6) and (3.7), but is not as accurate as Eq. (3.5) for intermediate values of τ and nonvanishing noise intensity.

The good agreement between theory, Eq. (3.5), and numerical determination of $\delta(\tau)$ is illustrated in Fig. 4 (see also Ref. 23). Our results prove that the approximate form (3.2) for $P_{st}(x;\tau)$ applies in the limit of very large noise correlation time as well. Such a trend is also apparent in Fig. 3 where, for $\tau=3.0$, a favorable comparison for $P_{st}(x;\tau)$ is restored in the stable regions about the potential minima.

Finally, in Fig. 5 we display the stationary distribution for the inverted potential $-f(x)$. The (absolute) values of parameters a, b, D, and τ are as in Fig. 3. The corresponding theoretical predictions (3.1)–(3.3) are also plotted for the sake of comparison. Due to the modified spatial symmetry of the system, the peak shift investigated above is now replaced by a shift of the relative minima of the stationary distribution. In principle, our discussion about the intrinsic limitations of the approximate predictions (3.1)–(3.3) applies to the inverted potential too, as illustrated in Fig. 5. However, the metastable nature of the inverted potential $-f(x)$ (see Fig. 1) seems to be reflected by the fact that all predictions overestimate the stationary distribution $P_{st}(x;\tau)$ at the potential maxima and underestimate the probability density about the (absolute) minima of the potential [Figs. 5(d)–5(f)]. Such a situation may also be responsible for the appearance of the bumps in Figs. 5(c) and 5(f) according to prediction (3.2). It should be noted, however, that a more favorable comparison of $P_{st}(x)$ predicted by the unified theory (3.2) may be achieved on employing a different normalization procedure. If prediction (3.2)—in addition to the previously used normalization—is fitted to the numerically exact peak height (MCF result) at $x=\pi$, the bumps at $x\approx 0,2\pi$ almost disappear. In conclusion, these plots confirm that the range of applicability of the theoretical predictions (3.1)–(3.3) is restricted to $D\ll\Delta f(0)$ even for very small values of τ [Fig. 5(d)].

IV. MEAN FIRST-PASSAGE TIME PROBLEM

The problem of MFPT in bistable potentials driven by colored noise attracted the attention of several investiga-

tors.[10,12–19,22,24] The predictions proposed have been obtained by employing the very same procedure. One starts with one of the approximated bona fide FPE's given in Sec. I and then applies the Stratonovich formula for the MFPT in bistable potentials, $T(\tau)$, which in the limit $D \ll \Delta f(0)$ can be given the form[1]

$$T=\int_{-\infty}^{0} dx \frac{1}{P_{\rm st}(x;\tau)D(x;\tau)} \int_{-\infty}^{x} dy\, P_{\rm st}(y;\tau) . \tag{4.1}$$

Without going into many details (for a review of these methods see Ref. 16) the various predictions for the MFPT in bistable potentials may be summarized as follows:

$$T^{-1}(\tau)=T^{-1}(0)\exp(-\kappa\tau) . \tag{4.2}$$

According to the τ expansion of Refs. 7 and 8, κ turns out to depend only very weakly on D. For instance, the first-order τ correction to $T^{-1}(0)$ calculated in Ref. 12 has been *ad hoc* exponentiated[14] to yield

$$\kappa=\tfrac{1}{2}[f''(x_m)+|f''(0)|]+O(D\tau) . \tag{4.3}$$

A similar result might be obtained by means of the unified theory.[16] On making use of the decoupling ansatz, instead, Hänggi and co-workers[13] predict a strong D dependence of κ,

$$\kappa=\frac{\Delta f(0)}{D} f''(x_m)+O(D\tau) . \tag{4.4}$$

One should bear in mind that any estimate of $T(\tau)$ based on a combined use of a *bona fide* FPE for $P(x;t;\tau)$ and the Stratonovich formula (4.1) for the MFPT may be illegitimate (see Refs. 21 and 25). The full FPE (1.7) and (1.8), indeed, describes a two-dimensional problem. The two-variable distribution $P_{\rm st}(x,\epsilon)$ cannot be factorized

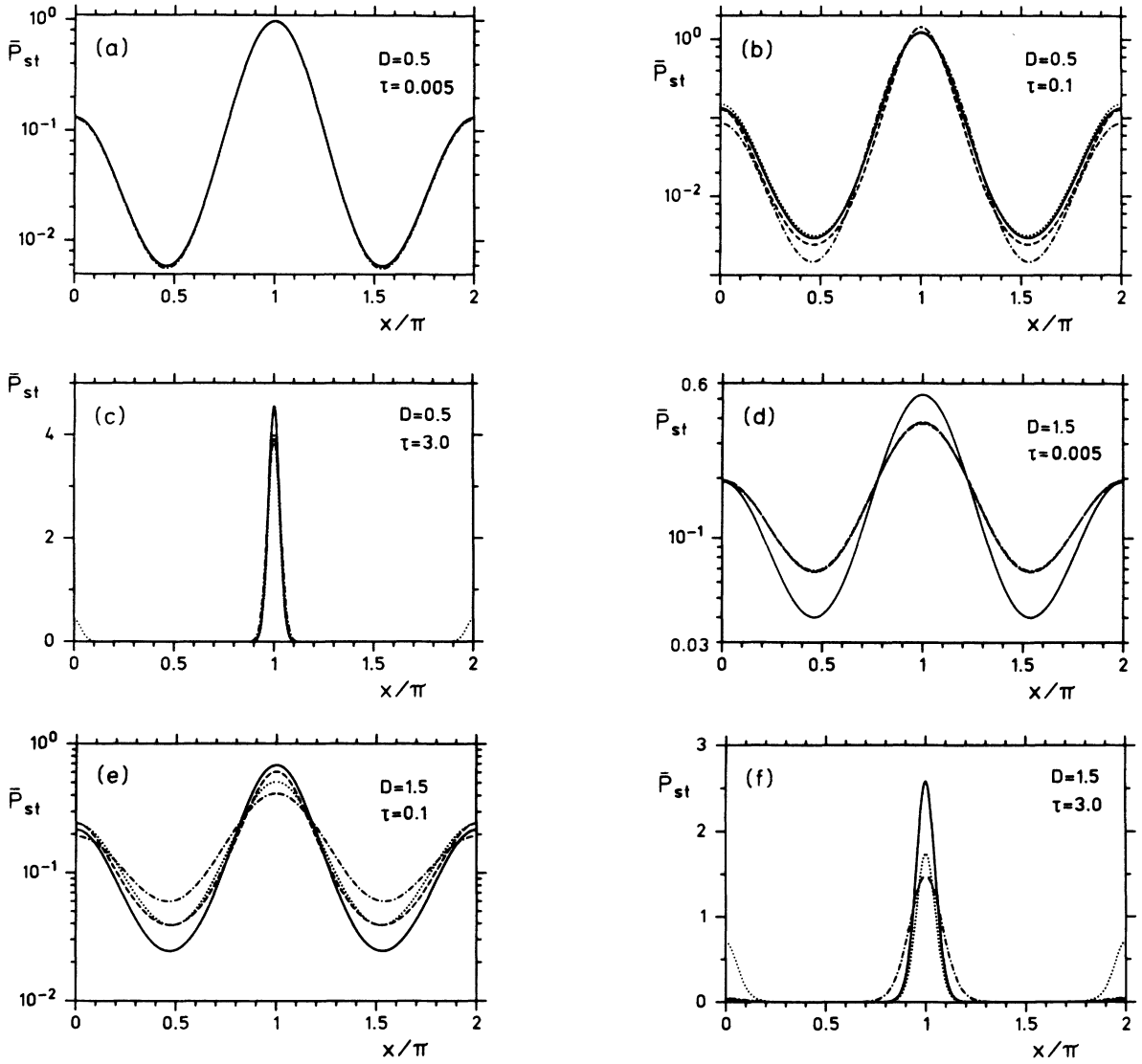

FIG. 5. (a)–(f), stationary distribution $P_{\rm st}(x;\tau)$ for the *metastable periodic* potential (2.2) with $a=-0.5$ and $b=-1$, i.e., $\Delta f(0)=\frac{49}{32}$, $\Delta f(\pi)/\Delta f(0)=\frac{81}{49}$. Solid curves, MCF result. Dotted curves, unified theory. Dashed curves, τ expansion. Dotted-dashed curves, decoupling ansatz. (c) and (f), linear scale; others, logarithmic scale.

into the product of two stationary distribution functions, one for the space coordinate and one for the auxiliary variable ϵ. As shown in a forthcoming paper,[21] the coupling between x and ϵ in the corresponding coordinate space (x,ϵ) is by no means negligible; otherwise stated, a truly non-Markovian theory is needed.[25] An alternative approach based on Kramers's original idea, extended to deal with colored noise, is worked out in Ref. 16. The relevant prediction for κ coincides with the sum of (4.3) and (4.4), namely,

$$\kappa=\frac{\Delta f(0)}{D}f''(x_m)+[f''(x_m)+|f''(0)|]/2+O(D\tau)\ . \tag{4.5}$$

As in Ref. 19, our numerical determination of MFPT is indirect. It is well known[1-3,26] that for high-potential barriers $D\ll\Delta f(0)$, the escape rate T^{-1} is accurately reproduced by the smallest nonvanishing eigenvalue $\lambda_1(\tau)$ of Eq. (2.4), which in turn can be calculated numerically by means of the MCF algorithm. Throughout the present section the identification $\lambda_1(\tau)=T^{-1}(\tau)$ is understood. Our results for $\lambda_1(\tau)$ are displayed in Fig. 6(a) for the double periodic cosine potential (2.2) ($a=0$) and in Fig. 6(b) for the periodic bistable potential $[\Delta f(\pi)\gg\Delta f(0)]$. In both cases some important features are immediately recognizable.

(i) $\lambda_1(\tau)$ decreases almost exponentially with τ for the whole interval of τ explored in close agreement with formula (4.2).

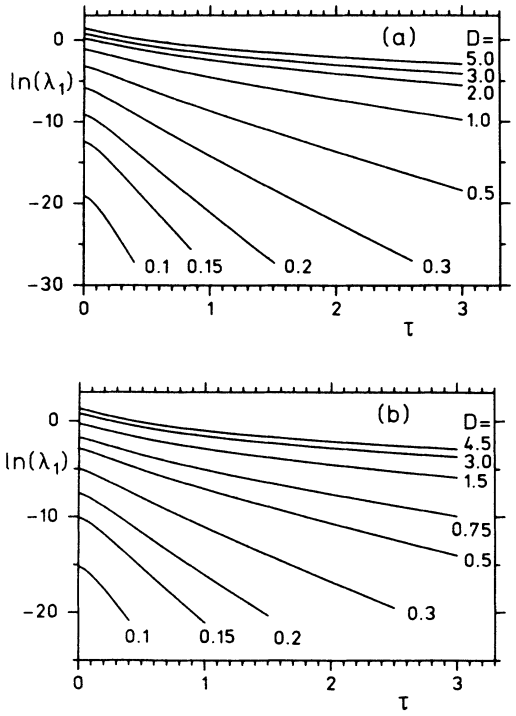

FIG. 6. MCF results for the first nonvanishing eigenvalue. (a) Cosine potential (2.2) with $a=0$ and $b=1$, i.e., $\Delta f(0)=\Delta f(\pi)=2$. (b) Bistable periodic potential (2.2) with $a=0.5$ and $b=1$, i.e., $\Delta f(0)=\frac{49}{32}$, $\Delta f(\pi)/\Delta f(0)=\frac{81}{49}$.

(ii) The slopes of the curves drawn in Fig. 6 exhibit a strong dependence on D. An increasingly stronger τ dependence shows up for higher-potential barriers, i.e., $\Delta f(0)\gg D$, whereas for small-potential barriers the curves obtained are almost parallel.

(iii) $\lambda_1(0)$ fits very closely the theoretical predictions available in the literature for both $\Delta f(0)\gg D$ (Kramers's theory) and $\Delta f(0)\ll D$ (see, eg., Chap. 11, Ref. 3), provided that the symmetry of the system is taken into account explicitly. A preliminary report of these results has been given in Ref. 19.

The escape rate $\lambda_1(\tau)$ in a periodic bistable potential can be determined by means of Kramers's theory, see Ref. 16. In Ref. 19, a rescaling of the noise correlation time τ in Eq. (4.2) has been invoked. Because, meanwhile, we know that such a rescaling is not justified rigorously by the periodicity of our potential, the factor $\frac{1}{4}$ introduced in Ref. 19 may be understood as an ad hoc factor replacing $\tau\to\tau/4$ in Eq. (4.2). Whether such a factor depends on the actual potential shape is a subject of further investigation. The dependence of $\ln[\lambda_1(\tau)]$ on τ/D, however, is in qualitative agreement with the predictions based on the decoupling Ansatz for moderate to large values of τ. For small values of D, $D\ll\Delta f(0)$, κ of Eq. (4.3) is negligible compared to κ of Eq. (4.4) and, therefore, the prediction based on the decoupling ansatz[13] equals the result of Eq. (4.5).

For the sake of comparison we report the analytical estimates of $\lambda_1(0)$ for several choices of the parameters. In the limit $D\ll\Delta f(0)$, Kramers's prediction is shown to hold good,

$$\lambda_1(0)=\frac{1}{\pi}[f''(x_m)|f''(0)|]^{1/2}\exp\left[\frac{-\Delta f(0)}{D}\right] \tag{4.6}$$

for the periodic bistable potential, while for the cosine potential ($a=\sigma$)

$$\lambda_1(0)=\frac{8b}{\pi}\exp\left[\frac{-2b}{D}\right]\ . \tag{4.7}$$

In both cases a suitable weight factor (2 and 4, respectively) has been introduced to account for the periodic multistability of the potential.[27] Since corrections proportional to $D/\Delta f(0)$ have been calculated explicitly (see, for instance, page 124, Ref. 3), an improved Kramers's rate[24] may be employed for $\lambda_1(0)$ in Fig. 6. According to the technique expounded in Ref. 3, paragraph 11.3, $\lambda_1(0)$ can also be determined analytically in the regime of a very-low-potential barrier,

$$\lambda_1(0)=D+\frac{a^2}{12D}\left[\left[\frac{a^2}{12D}\right]^2+b^2\right]^{1/2} \tag{4.8}$$

for the periodic bistable potential, and

$$\lambda_1(0)=D-b \tag{4.9}$$

for the cosine potential ($a=0$).

V. EIGENVALUE SPECTRUM OF THE INVERTED POTENTIAL

Let us now discuss an important property of the FPE (1.7). We wish to answer the question as to what happens when the potential $f(x)$ is inverted, $\bar{f}(x)=-f(x)$, *in the presence of colored noise.* We already know the answer for the case of white noise. The eigenvalue spectrum of the new FPE is essentially unchanged, the relevant eigenfunctions being analytically expressible in terms of the eigenfunctions of the initial FPE. As explained in Ref. 3, Sec. 5.8, the eigenvalues coincide exactly for periodic potentials with periodic boundary conditions of the type of Eq. (2.3). For a binding potential, where $f(x)$ tends to $+\infty$ at $x\to\pm\infty$, the inverted potential is a double-sided metastable potential, i.e., it tends to $-\infty$ at $x\to\pm\infty$. In such a case the stationary-state eigenvalue is deleted by inversion, while all of the other eigenvalues are unchanged when proper boundary conditions for $x\to\pm\infty$ are imposed. This means that we must assume reflecting walls for the original potential and absorbing walls for the metastable potential at $x\to\pm\infty$. [In the derivation of Ref. 3 it is tacitly assumed that $f(x)$ goes to infinity faster than $|x|$, so that the eigenvalue spectrum is discrete.] Finally, for a single-sided potential where $f(x)$ tends to $+\infty$ (or $-\infty$) for $x\to+\infty$ and to $-\infty$ (or $+\infty$) for $x\to-\infty$, the FPE for the inverted potential also restores the same eigenvalue spectrum.

In this section we want to prove that these results may be extended to a wide class of FPE's describing stochastic relaxation in one-dimensional potentials driven by colored noise, provided that the boundary conditions detailed above are imposed. The conjecture of isospectrality under potential inversion in the colored-noise case was guessed first from the numerical determination of λ_1 for the inverted periodic potential (2.2), see Fig. 1. Indeed, the eigenvalues λ_1 for the bistable and monostable periodic potentials coincide to within the round-off errors over the whole range of parameters a, b, D, and τ explored.

The proof runs as follows. We first remark that the eigenvalue equation corresponding to Eqs. (1.7) and (1.8) can be written in the form

$$-\lambda\Phi(x,\epsilon)=\mathbf{L}(x,\epsilon)\Phi(x,\epsilon)\ , \tag{5.1}$$

where the operator $\mathbf{L}(x,\epsilon)$ and the eigenfunctions $\Phi(x,\epsilon)$ are given by

$$\mathbf{L}(x,\epsilon)=\exp[f(x)/(2D)]\mathbf{L}_{\rm FP}\exp[-f(x)/(2D)]\ , \tag{5.2}$$

$$\Phi(x,\epsilon)=\exp[f(x)/(2D)]P(x,\epsilon)\ . \tag{5.3}$$

On introducing the creation and annihilation operators

$$\mathbf{a}^\dagger=-\sqrt{D}\,\frac{\partial}{\partial x}+\frac{f'(x)}{2\sqrt{D}},\quad \mathbf{a}=\sqrt{D}\,\frac{\partial}{\partial x}+\frac{f'(x)}{2\sqrt{D}}\ , \tag{5.4}$$

operator (5.2) can be cast into the form

$$\mathbf{L}(x,\epsilon)=-\mathbf{a}^\dagger\mathbf{a}-(\mathbf{a}^\dagger)^2+\mathbf{a}^\dagger\epsilon+\mathbf{L}_B(\epsilon)\ , \tag{5.5}$$

where $\mathbf{L}_B(\epsilon)$ denotes the bath operator (2.7). Analogously, for the inverted potential, Eq. (5.1) is replaced by

$$-\bar{\lambda}\bar{\Phi}(x,\epsilon)=\bar{\mathbf{L}}(x,\epsilon)\bar{\Phi}(x,\epsilon)\ , \tag{5.6}$$

with

$$\bar{\mathbf{L}}(x,\epsilon)=-\bar{\mathbf{a}}^\dagger\bar{\mathbf{a}}-(\bar{\mathbf{a}}^\dagger)^2+\bar{\mathbf{a}}^\dagger\epsilon+\mathbf{L}_B(\epsilon)\ . \tag{5.7}$$

After inverting the potential in Eq. (5.4), we easily realize that the creation and annihilation operators for the inverted problem can be expressed in terms of the corresponding operators of the initial problem, according to

$$\bar{\mathbf{a}}^\dagger=-\mathbf{a},\quad \bar{\mathbf{a}}=-\mathbf{a}^\dagger\ . \tag{5.8}$$

Thus we may write (5.7) in the form

$$\bar{\mathbf{L}}(x,\epsilon)=-\mathbf{a}\mathbf{a}^\dagger-\mathbf{a}^2-\mathbf{a}\epsilon+\mathbf{L}_B(\epsilon)\ . \tag{5.9}$$

By comparing Eq. (5.9) with the x adjoint of operator (5.5),

$$\mathbf{L}^\dagger(x,\epsilon)=-\mathbf{a}^\dagger\mathbf{a}-\mathbf{a}^2+\mathbf{a}\epsilon+\mathbf{L}_B(\epsilon)\ , \tag{5.10}$$

we obtain the key relation

$$\mathbf{a}\mathbf{L}^\dagger(x,-\epsilon)=\bar{\mathbf{L}}(x,\epsilon)\mathbf{a}\ . \tag{5.11}$$

[In the white-noise case $\mathbf{L}(x)=\mathbf{L}^\dagger(x)$ is an Hermitian operator and Eq. (5.11) simplifies to $\mathbf{a}\mathbf{L}=\bar{\mathbf{L}}\mathbf{a}$.] As already mentioned in Sec. I the eigenvalue spectrum cannot depend on the sign of ϵ. Since any operator and its adjoint are isospectral, Eq. (5.1) yields

$$-\lambda\Phi^\dagger(x,-\epsilon)=\mathbf{L}^\dagger(x,-\epsilon)\Phi^\dagger(x,-\epsilon)\ . \tag{5.12}$$

Applying the annihilation operator $\mathbf{a}$ to both sides of Eq. (5.12) and making use of Eq. (5.11) we prove that $\mathbf{a}\Phi^\dagger(x,\epsilon)$ is an eigenfunction of $\bar{\mathbf{L}}$ [see Eq. (5.6)] with the same eigenvalue λ, i.e.,

$$\bar{\lambda}=\lambda,\quad \bar{\Phi}(x,\epsilon)\sim\mathbf{a}\Phi^\dagger(x,-\epsilon)\ , \tag{5.13}$$

provided that $\mathbf{a}\Phi^\dagger(x,-\epsilon)$ is not identically zero. For the stationary eigenvalue $\lambda=0$ the adjoint eigenfunction $P_{\rm st}^\dagger(x,\epsilon)$ is a constant and $\Phi^\dagger(x,\epsilon)$ is proportional to $\exp[f(x)/(2D)]$. Thus, $\mathbf{a}\Phi^\dagger$ vanishes and nothing can be said about the eigenfunction of the inverted problem. Of course, a stationary solution will always exist in the inverted potential problem with periodic boundary conditions. On the contrary, the inverted problem of a binding potential with natural boundary conditions cannot have a stationary solution.

The proof above can be extended to any noise statistics represented by a linear thermal bath operator

$$\mathbf{L}_B(\epsilon,\epsilon_1,\ldots,\epsilon_N)\ ,$$

where $\epsilon,\epsilon_1,\ldots,\epsilon_N$ are $N+1$ auxiliary variables. Thus all the properties of the white-noise FPE (1.3) stated in the beginning of this section are also valid if the noise is colored.

Finally, we note that the isospectrality of the inverted Fokker-Planck potentials can be given a simple supersymmetric interpretation. The Fokker-Planck operator $\mathbf{L}_{\rm FP}(x,\epsilon)$ was associated with a non-Hermitian Hamiltonian operator $\mathbf{L}(x,\epsilon)$ which defines two complete sets of orthogonal functions $\{\Phi_n\}$ and $\{\Phi_n^\dagger\}$. Inverting the potential in the FPE left the eigenvalue spectrum unchanged—apart from possibly deleting the zero eigenvalue. This operation corresponds to transforming

$\mathbf{L}(x,\epsilon)$ according to the generalized supersymmetric description $\mathbf{a}\rightarrow -\mathbf{a}^{\dagger}$ and $\mathbf{a}^{\dagger}\rightarrow -\mathbf{a}$. The eigenfunctions of the non-Hermitian supersymmetric partner $\bar{\mathbf{L}}(x,\epsilon)$ are given by $\mathbf{a}\Phi_n^{\dagger}$. The similarity to ordinary supersymmetry for Hamiltonian operators is apparent.[28,29]

VI. CONCLUSIONS

It was our intention throughout the numerical investigation reported above to discriminate among a number of conflicting theoretical analyses elaborated by several groups over the last ten years. The only conclusion we feel able to draw at this stage of our understanding, however, is that most of those authors did grasp some important features of the problem under study, but a satisfactory and exhaustive theory of bistability in the presence of colored noise lies beyond the reach of the theoretical tools employed to date.

ACKNOWLEDGMENTS

We wish to thank the Alexander von Humboldt Stiftung, the Deutsche Forschungsgemeinschaft, and the Istituto Nazionale di Fisica Nucleare for financial support. Useful discussions with Professor P. Hänggi and Dr. P. Jung are also gratefully acknowledged.

APPENDIX: MATRIX CONTINUED FRACTION ALGORITHM

The basic ingredients of the MCF algorithm have already been outlined in Sec. II. The eigenvalue problem (2.4) is solved by expanding the stationary two-dimensional distribution $P_{\rm st}(x,\epsilon)$ into two suitable sets of orthogonal functions of x and ϵ, respectively. The expansion sets are chosen in order to satisfy the natural boundary conditions for ϵ (Hermite functions) and the periodicity condition (2.3) for x (Fourier series). We also exploit the symmetry of the FPE (1.7), $\mathbf{L}_{\rm FP}(x,\epsilon)=\mathbf{L}_{\rm FP}(-x,-\epsilon)$, which allows us to take either the even or the odd part of $P(x,\epsilon)$, depending on the quantity we want to compute. Next, we make the differential operator $\mathbf{L}_{\rm FP}$ operate on $P^{e,o}(x,\epsilon)$ and introduce a suitable vector notation $\mathbf{c}_m=\{c_m^n\}$. Reordering the expansion terms leads to the tridiagonal vector recurrence relation (2.8)

$$\mathbf{Q}_m^{+}\mathbf{c}_{m+1}+\mathbf{Q}_m\mathbf{c}_m+\mathbf{Q}_m^{-}\mathbf{c}_{m-1}=0\ . \tag{A1}$$

The simple tridiagonal structure of Eq. (A1) is due to our choice of the set of orthonormal ϵ functions. Both the expansions in the odd and in the even eigenfunctions (2.6) can be cast into a tridiagonal vector recurrence relation. The matrices in Eq. (A1) for $P^{o}(x,\epsilon)$ are given the form

$$\begin{aligned}(\mathbf{Q}_m^{+})_{n,n'}&=-(\mathbf{Q}_{m+1}^{-})_{n,n'}\\&=(-1)^m\sqrt{(D/\tau)(m+1)}\,n\,\delta_{n,n'}\ ,\\(\mathbf{Q}_m)_{n,n'}&=\left[\lambda-\frac{m}{\tau}\right]\delta_{n,n'}-\frac{an}{2}(\delta_{n+1,n'}-\delta_{n-1,n'})\\&\quad+bn(\delta_{n+2,n'}-\delta_{n-2,n'})+(-1)^m\delta_{n,1}\ ,\end{aligned} \tag{A2}$$

while for $P^{e}(x,\epsilon)$ the term $(-1)^m$ has to be replaced by $(-1)^{m+1}$. On defining the matrices $\mathbf{K}_m$, $\mathbf{K}_m\mathbf{c}_m\equiv\mathbf{Q}_m^{+}\mathbf{c}_{m+1}$, we solve Eq. (A1) for $m=0$,

$$[\mathbf{Q}_0(\lambda)+\mathbf{K}_0(\lambda)]\mathbf{c}_0=\mathbf{0}\ . \tag{A3}$$

The matrix $\mathbf{K}_0(\lambda)$ is expressed through a MCF expansion[3]

$$\mathbf{K}_0(\lambda)=-\mathbf{Q}_0^{+}\cfrac{1}{\mathbf{Q}_1(\lambda)-\mathbf{Q}_1^{+}\cfrac{1}{\mathbf{Q}_2(\lambda)-\mathbf{Q}_2^{+}\cfrac{1}{\mathbf{Q}_3(\lambda)-\cdots}\mathbf{Q}_3^{-}}\mathbf{Q}_2^{-}}\mathbf{Q}_1^{-}\ , \tag{A4}$$

where each fraction line denotes a matrix inversion. (For an alternative approach to colored-noise problems by means of MCF's, see Ref. 30.)

From Eq. (A3) we can calculate the (discrete) eigenvalue spectrum (see Fig. 6) by solving the determinantal equation

$$\det[\mathbf{Q}_0(\lambda)+\mathbf{K}_0(\lambda)]=0\ . \tag{A5}$$

In the stationary case, $\lambda=0$, one immediately recognizes that the determinant (A5) vanishes and the unique solution $\mathbf{c}_0$ to the homogeneous equation (A3) determines the one-dimensional stationary distribution $P_{\rm st}(x;\tau)$ (after integration over the auxiliary variable ϵ). The computation of the two-dimensional eigenfunctions requires a greater numerical effort.[21] The accuracy of the MCF algorithm has to be tested for a suitable choice of the matrix size N and the iteration number M. All calculations reported herein were done in double precision (see, e.g., the quite remarkable range of λ values covered in Fig. 6) with 50×50 matrices and 150 iterations of the MCF.

*On leave from Dipartimento di Fisica dell' Universita and Istituto Nazionale di Fisica Nucleare, I-06100 Perugia, Italy.

[1]R. L. Stratonovich, *Topics in the Theory of Random Noise* (Gordon and Breach, New York, 1967), Vol. I.

[2]H. Haken, *Synergetics* (Springer, Berlin, 1983).

[3]H. Risken, *The Fokker-Planck Equation* (Springer, Berlin, 1984).

[4]H. A. Kramers, Physica 7, 284 (1940).

[5]T. Fonseca, J. A. M. F. Gomes, P. Grigolini, and F. Marchesoni, Adv. Chem. Phys. **62**, 389 (1985); for a review see, e.g., P. Hänggi, J. Stat. Phys. **42**, 105 (1986).

[6]J. S. Langer, Ann. Phys. (Leipzig) **54**, 258 (1969); R. F. Grote and J. T. Heynes, J. Chem. Phys. **73**, 2715 (1980); B. Carmeli and A. Nitzan, Phys. Rev. Lett. **49**, 423 (1982); K. Vogel, H. Risken, W. Schleich, M. James, F. Moss, and P. V. E. McClintock, Phys. Rev. A **35**, 463 (1987); P. Lett, E. C. Gage, and T. H. Chyba, *ibid.* **35**, 746 (1987); R. F. Fox and R. Roy, *ibid.* **35**, 1838 (1987); T. Leiber, P. Jung, and H. Risken, Z. Phys. B **66**, 397 (1987).

[7]M. Lax, Rev. Mod. Phys. **38**, 541 (1966); R. L. Stratonovich, *Topics in the Theory of Random Noise* (Gordon and Breach, New York, 1967), Vol. II; N. G. van Kampen, Phys. Rep. **24C**, 171 (1976); J. M. Sancho, M. San Miguel, S. L. Katz, and J. D. Gunton, Phys. Rev. A **26**, 1589 (1982); J. M. Sancho, M. San Miguel, H. Yamozaki, and T. Kawakubo, Physica **116A**, 560 (1982); K. Lindenberg and B. J. West, Phys. Rev. A **128**, 205 (1984).

[8]P. Grigolini and F. Marchesoni, Adv. Chem. Phys. **62**, 29 (1985).

[9]L. Schimansky-Geier, A. V. Tolstopjatenko, and W. Ebeling, Phys. Lett. **108A**, 329 (1985); H. Malchow and L. Schimansky-Geier, *Noise and Diffusion in Bistable Nonequilibrium Systems* (Teubner, Berlin, 1985), Vol. 5, pp. 83–87; V. Altares and G. Nicolis, J. Stat. Phys. **46**, 191 (1987).

[10]R. F. Fox, Phys. Rev. A **33**, 467 (1986); **34**, 4525 (1986); the authors believe that the preceding two papers contain some confusing arguments; see R. F. Fox, Phys. Rev. A **37**, 911 (1988).

[11]P. Jung and P. Hänggi, Phys. Rev. A **35**, 4464 (1987).

[12]P. Hänggi, F. Marchesoni, and P. Grigolini, Z. Phys. B **56**, 333 (1984).

[13]P. Hänggi, T. J. Mroczkowski, F. Moss, and P. V. E. McClintock, Phys. Rev. A **32**, 695 (1985); L. Fronzoni, P. Grigolini, P. Hänggi, F. Moss, R. Mannella, and P. V. E. McClintock, *ibid.* **33**, 3320 (1986); K. Vogel, T. Leiber, H. Risken, P. Hänggi, and W. Schleich, *ibid.* **35**, 4882 (1987).

[14]J. Masoliver, B. J. West, and K. Lindenberg, Phys. Rev. A **35**, 3086 (1987).

[15]J. M. Sancho, F. Sagues, and M. San Miguel, Phys. Rev. A **33**, 3399 (1986).

[16]F. Marchesoni, Phys. Rev. A **36**, 4050 (1987).

[17]S. Chaturvedi and F. Shibata, Z. Phys. B **35**, 297 (1979).

[18]P. Jung and H. Risken, Z. Phys. B **61**, 367 (1985).

[19]T. Leiber, F. Marchesoni, and H. Risken, Phys. Rev. Lett. **59**, 1381 (1987); **60**, 659(E) (1988).

[20]H. Haken, J. A. S. Kelso, and H. Bunz, Biol. Cybern. **51**, 347 (1985); J. P. Scholz, J. A. S. Kelso, and G. Schöner, Phys. Lett. A **123**, 390 (1987).

[21]T. Leiber, F. Marchesoni, and H. Risken (unpublished).

[22]P. Jung and P. Hänggi (unpublished).

[23]P. Jung and P. Hänggi, Bull. Am. Phys. Soc. **32**, 417 (1987).

[24]T. Leiber and H. Risken (unpublished).

[25]P. Hänggi and P. Talkner, Phys. Rev. A **32**, 1934 (1985).

[26]P. Talkner, Z. Phys. B **68**, 201 (1987).

[27]F. Marchesoni, Phys. Rev. B **32**, 1827 (1985).

[28]C. M. Bender, F. Cooper, and B. Freedman, Nucl. Phys. **B219**, 61 (1983); M. Bernstein and L. S. Brown, Phys. Rev. Lett. **52**, 1933 (1984).

[29]For a review see, e.g., B. Freedman and F. Cooper, Physica **15D**, 138 (1985).

[30]K. Wodkiewicz, Z. Phys. B **42**, 95 (1981).